Relaxation of Shannon entropy for trapped interacting bosons with dipolar interactions

Sangita Bera[1], Sudip Kumar Haldar[2,3,4], Barnali Chakrabarti[1,5,a], Andrea Trombettoni[6,7], and V. K. B. Kota[8]

[1] Department of Physics, Presidency University, 86/1 College Street, Kolkata 700073, India
[2] Department of Physics, SRM University Delhi-NCR, Plot No. 39 Rajiv Gandhi education city, Sonipat 131029, India
[3] Haifa Research Center for Theoretical Physics and Astrophysics, University of Haifa, Haifa 3498838, Israel
[4] Department of Mathematics, University of Haifa, Haifa 3498838, Israel
[5] The Abdus Salam International Center for Theoretical Physics, 34100 Trieste, Italy
[6] CNR-IOM DEMOCRITOS Simulation Center, Via Bonomea, 265, 34136, Trieste, Italy
[7] Scuola Internazionale di Studi Avanzati (SISSA) and INFN, Sezione di Trieste, Via Bonomea 265, 34136 Trieste, Italy
[8] Physical Research Laboratory, Navrangpura, Ahmedabad 380009, India

Abstract. We study the quantum many-body dynamics and entropy production triggered by an interaction quench of few dipolar bosons in an external harmonic trap. We solve the time-dependent many-body Schrödinger equation by using an in-principle numerically exact many-body method called the multiconfigurational time-dependent Hartree method for bosons (MCTDHB). We study the dynamical measures with high level of accuracy. We monitor the time evolution of the occupation in the natural orbitals and normalized first- and second-order Glauber's correlation functions. In particular, we focus on the relaxation dynamics of the Shannon entropy. Comparison with the corresponding results for contact interactions is presented. We observe significant effects coming from the presence of the non-local part of the dipolar interaction. The relaxation process is very fast for dipolar bosons with a clear signature of a truly saturated maximum entropy state. We also discuss the connection between the entropy production and the occurrence of correlations and loss of coherence in the system. We identify the long-time relaxed state as a many-body state retaining only diagonal correlations in the first-order correlation function and building up anti-bunching effect in the second-order correlation function.

1 Introduction

The investigation of nonequilibrium quantum dynamics has been stimulated by the remarkable progress in experimental techniques. Ultracold atomic gases and trapped ions are a test-bed for such studies as they offer a very good isolation from the environment [1–9]. A forefront research in this direction aims at characterizing the dynamical properties of isolated quantum many-body systems [9–14]. In this context, the onset of thermalization in isolated quantum systems caused by the interparticle interaction has received great interest [15–25]. The necessary condition for the thermalization is the statistical relaxation of the isolated system to equilibrium. In some recent studies [26–35] the viability of thermalization has been associated with the onset of quantum chaos. The latter in systems of interacting Fermi or Bose particles implies a pseudorandomness depending mainly on the strength of the interparticle interaction. In the recent study of interacting spin $\frac{1}{2}$ system, the delocalization of

the eigenstates in the energy shell approach was investigated [12,13]. The eigenstate thermalization hypothesis (ETH) [36–38] predicts that the expectation value of few-body observable should correspond to the prediction of microcanonical ensemble [39–42]. The recent works [43,44] make a clear connection between the ETH and information entropy. Although a vast amount of works exist to characterize the delocalized eigenstates and its connection with the statistical relaxation, many open questions which still are studied:

a) How and in which timescale the system relaxes?
b) How the time evolution of the entropy and the onset of statistical relaxation are connected?
c) What is the link between the production of entropy and both the build up of correlations and the loss of coherence?
d) What is the effect of long-range interactions?

The last question (d) is motivated by the fact that many investigations have focused on contact/short-range investigations. In this respect it would be interesting to compare results for long-range interactions with short-range

findings and with recent results for quantum systems with long-range couplings [45–55]. Ultracold atoms with dipole-dipole interactions are a popular setup to investigate the effect of non-local interactions [56]. Dipolar atoms in quasi-one-dimensional traps can be experimentally realized and provide a tool to explore a rich manybody physics [57,58]. It is important to point out that one can realize also several coupled one-dimensional systems, with a tunable couplings [59].

In this paper, we focus on the role of dipolar interaction in the relaxation dynamics of interacting bosons in a 1D harmonic oscillator (HO) trap. The comparison between the short-range contact interactions and long-range dipolar ones is also presented. Ultracold dilute Bose gases are very often well described by the contact interaction, defined as

$$\hat{V}(x_i - x_j) = \lambda \delta(x_i - x_j), \tag{1}$$

where the dimensionless parameter λ is the strength of the 1D contact interaction [60]. For dipolar interaction, in quasi-1D geometries, the effective non-local two-body interaction term V can be obtained by integrating over the transverse directions [61]. Here we consider dipolar interaction of the form

$$\hat{V}(x_i - x_j) = \frac{g_d}{|x_i - x_j|^3 + \alpha}, \tag{2}$$

where the dimensionless parameter g_d is the strength of interaction and α is the short-scale cut-off to regularize the divergence at $x_i = x_j$. We solve the N body Schrödinger equation with very high level of accuracy using the multiconfigurational time-dependent Hartree method for bosons (MCTDHB) [62–66], with the manybody ansatz being the sum of the different configurations of N particles distributed over M orbitals.

In our present setup, we consider N dipolar bosons in 1D HO trap. We consider few particles, such as $N = 4$, even though we checked that the obtained results are consistent with findings for higher number of particles, such $N \sim 6$. Our procedure corresponds to have the non-interacting system at $t < 0$ and then at time $t = 0$ perform a quantum quench from $g_d = 0$ to a finite, possibly large, value of g_d. Quantum quenches of the 1D Bose gas with contact interactions have been deeply investigated in the literature [67–78]. The results obtained with the dipolar interactions are further compared with the quantum quench for the contact interaction. The relaxation is studied by analyzing the time evolution of Shannon information entropy and as well the normalized first- and second-order Glauber's correlation functions. The contrast between contact and dipolar interactions is demonstrated by the timescale of relaxation process. We observe interesting many-body properties in the time evolution of first- and second-order correlation functions in the case of dipolar interactions. We also demonstrate that the observed relaxation is associated with the loss of coherence in the first-order correlation function and the occurrence of an *anti-bunching* effect in the second-order correlation function. The effect of long-range repulsive tail of the dipolar interaction makes the dynamics very interesting. The corresponding entropy evolution shows sharp linear

increment at very short time and then saturation. The first-order correlation is quickly lost as well as a clear anti-bunching effect is quickly developed for the dipolar interaction.

Since the high resolution image technique allows to probe the spatial correlation functions [79,80], the observations made in the present manuscript could be verified in future experiments.

The paper is organized as follows. In Section 2, we give a brief description of Hamiltonian and the used numerical method. In Section 3, we introduce the key quantities that are subsequently analyzed. In Section 4 we present our results for the post-quench dynamics. Section 5 provides a summary and discussion of our results.

2 Methodology

The dynamics of a system of N interacting structureless bosons in a one-dimensional (1D) harmonic well is governed by the time-dependent many-body Schrödinger equation:

$$i\frac{\partial \Psi}{\partial t} = \hat{H}\Psi. \tag{3}$$

The total Hamiltonian we consider is

$$\hat{H}(x_1, x_2, \ldots, x_N) = \sum_{j=1}^{N} \hat{h}(x_j) + \Theta(t) \sum_{k>j=1}^{N} \hat{V}(x_j - x_k). \tag{4}$$

Here x_j is the coordinate of the j-th boson, $\hat{h}(x) = \hat{T}(x) + \hat{V}_T(x)$ is the one-body Hamiltonian containing kinetic energy $T(x) = -\frac{1}{2}\frac{\partial^2}{\partial x^2}$ and a harmonic well trapping potential $V_T(x) = \frac{1}{2}x^2$ terms. In this work, we have chosen $\hbar = m = \omega = 1$ to calculate all the quantities in dimensionless unit. The pairwise interaction between the j-th and k-th bosons is given by $\hat{V}(x_j - x_k)$. The Heaviside step function $\Theta(t)$ indicates the interaction quench at $t = 0$. In this work, we have considered dipolar interaction $\hat{V}(x_i - x_j) = \frac{g_d}{|x_i - x_j|^3 + \alpha}$. Also, we considered contact δ-potential for comparison.

The time-dependent many-body Schrödinger equation can not be solved directly except only for a few specific cases, see, e.g., [81]. Thus equation (3) is solved by an in-principle numerically exact many-body method called the multi-configurational time-dependent Hartree method for bosons (MCTDHB), [62–64] which has been benchmarked with an exactly-solvable model [82,83]. This method has already been extensively used in the literature [84–99]. Detailed derivation of the MCTDHB equation of motions can be found in [63]. For completeness, we provide here with a brief description of the method.

In MCTDHB, the ansatz for solving equation (3) is obtained by the superposition of all possible $\binom{N + M - 1}{N}$ time-dependent permanents, obtained by distributing N bosons in M time-dependent single-particle orbitals $\{\phi_k(\mathrm{x}, t)\}$. Therefore

$$|\Psi(t)\rangle = \sum_{\boldsymbol{n}} C_{\boldsymbol{n}}(t) |\boldsymbol{n}; t\rangle, \tag{5}$$

where the summation runs over all the occupations $\boldsymbol{n} = (n_1, n_2, \cdots, n_M)$ such that these preserve total number of bosons N, i.e., $n_1 + n_2 + \cdots + n_M = N$ and the time-dependent permanents are given by

$$
\begin{aligned}
|\boldsymbol{n}; t\rangle = &\frac{1}{\sqrt{n_1! n_2! \cdots n_M!}} \\
&\times \left(b_1^\dagger(t)\right)^{n_1} \left(b_2^\dagger(t)\right)^{n_2} \cdots \left(b_M^\dagger(t)\right)^{n_M} |vac\rangle,
\end{aligned} \quad (6)
$$

where $|vac\rangle$ is the vacuum. The bosonic annihilation and corresponding creation operators obey the usual commutation relations $b_k(t) b_j^\dagger(t) - b_j^\dagger(t) b_k(t) = \delta_{kj}$ at any point in time. Note that in representation (5) both the expansion coefficients $\{C_{\boldsymbol{n}}(t)\}$ and orbitals $\{\phi_k(\mathrm{x}, t)\}$ comprising the permanents $|\boldsymbol{n}; t\rangle$ are independent parameters. We point out that because of the time-dependent permanents, one can use a much shorter expansion in equation (5) compared to the ansatz with fixed time-independent orbitals.

For an exact theory, M should be infinitely large. However, for numerical computations one has to truncate the series at a finite M. In actual calculations, we keep on increasing M until we reach the convergence with respect to M and thereby we obtain a numerically-exact result. Here we would like to point out that for $M = 1$, the ansatz equation (5) gives back the ansatz for the Gross Pitaevskii theory [100,101]. To solve for the time-dependent wave-function $\Psi(t)$ we employ the usual Lagrangian formulation of the time-dependent variational principle [102,103] subject to the orthonormality between the orbitals. In this framework, substitution of the many-body *ansatz* equation (5) for $\Psi(t)$ into the functional action of the time-dependent Schrödinger equation and the requirement of the stationarity of the functional action with respect to its arguments $\{C_{\boldsymbol{n}}(t)\}$ and $\{\phi_k(\mathrm{x}, t)\}$ lead to the working equations of the MCTDHB:

$$
i \left| \dot{\phi}_j \right\rangle = \hat{\mathbf{P}} \left[\hat{h} \left| \phi_j \right\rangle + \sum_{k,s,q,l=1}^{M} \{\rho(\mathbf{t})\}_{jk}^{-1} \rho_{ksql} \hat{W}_{sl} \left| \phi_q \right\rangle \right];
$$

$$
\hat{\mathbf{P}} = 1 - \sum_{j'=1}^{M} \left| \phi_{j'} \right\rangle \left\langle \phi_{j'} \right|
$$

$$
\mathbf{H}(t) \mathbf{C}(t) = i \frac{\partial \mathbf{C}(t)}{\partial t}. \quad (7)
$$

Here, $\rho(\mathbf{t})$ is the reduced one-body density matrix (see Eq. (8) below), ρ_{ksql} are the elements of the two-body reduced density matrix (see Eq. (9) below), and $\mathbf{H}(t)$ is the Hamiltonian matrix with the elements $H_{\boldsymbol{nn'}}(t) = \left\langle \boldsymbol{n}; t \left| \hat{H} \right| \boldsymbol{n'}; t \right\rangle$.

It is convenient to define the different quantities of interest in terms of the one-body and the two-body reduced density matrices [104–107] instead of the full many-body wavefunction. Given the normalized many-body wavefunction $\Psi(t)$, the reduced one-body density matrix can be calculated as

$$
\begin{aligned}
\rho^{(1)}(x_1 | x_1'; t) = &N \int dx_2 \ldots dx_N \, \Psi^*(x_1', x_2, \ldots, x_N; t) \\
&\times \Psi(x_1, x_2, \ldots, x_N; t) \\
= &\sum_{j=1}^{M} n_j(t) \, \phi_j^{*NO}(x_1', t) \phi_j^{NO}(x_1, t). \quad (8)
\end{aligned}
$$

Here, $\phi_j^{NO}(x_1, t)$ are the time-dependent natural orbitals and $n_j(t)$ the time-dependent natural occupation numbers. The natural occupations $n_j(t)$ are used to characterize the (time varying) degree of condensation in a system of interacting bosons [108] and satisfy $\sum_{j=1}^{M} n_j = N$. If only one macroscopic eigenvalue $n_1(t) \approx \mathcal{O}(N)$ exists, the system is condensed [108] whereas if there are more than one macroscopic eigenvalues, the BEC is said to be fragmented [109–112]. The diagonal of the $\rho^{(1)}(x_1 | x_1'; t)$ gives the density of the system $\rho(x; t) \equiv \rho^{(1)}(x | x' = x; t)$.

Similarly, the two-body density can be calculated as

$$
\begin{aligned}
&\rho^{(2)}(x_1, x_2 | x_1', x_2'; t) \\
&= N(N-1) \int dx_3 \ldots dx_N \Psi^*(x_1', x_2', x_3, \ldots, x_N; t) \\
&\times \Psi(x_1, x_2, x_3, \ldots, x_N; t). \quad (9)
\end{aligned}
$$

Therefore, the matrix elements of the two-body reduced density matrix are given by $\rho_{ksql} = \left\langle \Psi \left| b_k^\dagger b_s^\dagger b_q b_l \right| \Psi \right\rangle$ where b_k and $b_k^\dagger$ are the bosonic annihilation and creation operators, respectively.

3 Key quantities

3.1 Shannon information entropy

Entropy of quantum system is a measure of degree of order in a particular state [13,38,113–116]. The Shannon information entropy (SIE) of the one-body density in position space is defined as

$$
S_x(t) = -\int dx \rho(x, t) \ln[\rho(x, t)]
$$

and similarly in the momentum space as

$$
S_k(t) = -\int dk \rho(k, t) \ln[\rho(k, t)]
$$

where $\rho(x)$ and $\rho(k)$ are the density of the system in coordinate space and in momentum space respectively [117–119]. The two SIEs as defined above are two independent key quantities in the calculation of quantum information in many-body system, as they measure the delocalization of the corresponding distributions. However, since SIE is based on the one-body density, one can not infer the presence of correlation in the many-body state. The concept of many-body information entropy is introduced in the Gaussian orthogonal ensemble (GOE) of random matrices [120]. In general, in the interaction

quench, when different entropy measures take the GOE values - is referred to as statistical relaxation.

In the present calculation, where the many-body ansatz is constructed from the time-dependent coefficients as well as time-dependent orbitals, we provide two alternative definitions of many-body information entropy. Information entropy which is calculated from the time-dependent coefficients is termed as coefficient Shannon information entropy (C-SIE or $S^{\text{info}}(t)$) and calculated as

$$S^{\text{info}}(t) = -\sum_{\boldsymbol{n}} |C_{\boldsymbol{n}}(t)|^2 \ln |C_{\boldsymbol{n}}(t)|^2, \qquad (10)$$

where

$$\begin{aligned} |C_{\boldsymbol{n}}(t)|^2 = \frac{1}{\prod_{i=1}^{M} n_i!} \langle \Psi | [b_1(t)]^{n_1} ... [b_M(t)]^{n_M} \\ \times [b_1^{\dagger}(t)]^{n_1} ... [b_M^{\dagger}(t)] n_M | \Psi \rangle. \end{aligned} \qquad (11)$$

Thus, $S^{\text{info}}(t)$ is the measure of effective number of basis states that contribute to a given many-body state $|\Psi(t)\rangle$ at time t. Alternatively, the measure of $S^{\text{info}}(t)$ can be directly linked with the distribution of coefficients in the Hilbert space. In GP mean-field [100,101] and multiorbital mean-field theory [121] as a single contribution is included $S^{\text{info}}(t) = 0$ for all time. Thus, $S^{\text{info}}(t)$ can not be produced in mean-field theory.

From the time-dependent orbitals, we define occupation Shannon information entropy (O-SIE or $S^{\text{occu}}(t)$) and calculated from

$$S^{\text{occu}}(t) = -\sum_{j} n_j \ln n_j. \qquad (12)$$

Thus, $S^{\text{occu}}(t)$ is an entropy obtained from the natural occupations i.e., the eigenvalues of the reduced one-body density matrix $\bar{n}_j = \frac{n_j}{N}$. For time-dependent GP, $S^{\text{occu}}(t) = 0$ for all time, as only one natural occupation $\bar{n}_1 = \frac{n_1}{N}$ is included and can not be produced in mean-field theory.

3.2 Correlation functions

To complement the results for the entropies $S^{\text{info}}(t)$ and $S^{\text{occu}}(t)$ we calculate the normalized first- and second-order Glauber's correlation functions at many-body level. The time evolution of the correlation function quantifies the coherence and fringe visibility in interference experiments. We demonstrate a fundamental relation between the production of many-body information entropy, the build-up of correlation and loss of coherence. We establish that loss of coherence is related with the increase in many-body entropy. As spatial correlation function can be directly measured, the observed findings can be scrutinized in the future experiments. The normalized p-th order correlation function is defined as

$$g^{(p)}(x_1', ..., x_p', x_1, ..., x_p; t) = \qquad (13)$$
$$\frac{\rho^{(p)}(x_1, ..., x_p | x_1', ..., x_p'; t)}{\sqrt{\prod_{i=1}^{p} \rho^{(1)}(x_i | x_i; t) \rho^{(1)}(x_i' | x_i'; t)}}.$$

It is the key quantity to define the spatial p-th order coherence. Here, $\rho^{(p)}(x_1, ..., x_p | x_1', ..., x_p'; t)$ is the p-th order reduced density matrix of the state $|\Psi\rangle$ [122]. In the case of $|g^{(p)}(x_1..., x_p, x_1..., x_p; t)| > 1 \, (< 1)$, the detection probabilities of p particles at positions $x_1, ..., x_p$ are referred to as (anti-)correlated. The normalized first-order coherence is directly related to the fringe visibility in interference experiments and it is defined as

$$g^{(1)}(x_1', x_1; t) = \frac{\rho^{(1)}(x_1' | x_1; t)}{\sqrt{\rho(x_1'; t) \rho(x_1; t)}}, \qquad (14)$$

$g^{(1)}(x_1', x_1; t) < 1$ means the visibility of interference fringes in the experiment is less than 100%, which is referred to as loss of coherence. At variance, $g^{(1)}(x_1', x_1; t) = 1$ corresponds to maximal fringe visibility and is referred to as full coherence. The diagonal of the two-body density matrix (Eq. (9)) is given by,

$$\rho^{(2)}(x_1, x_2; t) \equiv \rho^{(2)}(x_1' = x_1, x_2' = x_2 | x_1, x_2; t). \qquad (15)$$

The diagonal of the second-order correlation function $g^{(2)}(x_1' = x_1, x_2' = x_2 | x_1, x_2; t) = g^{(2)}(x_1, x_2; t)$ is calculated from

$$g^{(2)}(x_1, x_2; t) = \frac{\rho^{(2)}(x_1, x_2; t)}{\rho(x_1; t) \rho(x_2; t)}, \qquad (16)$$

when $g^{(2)} < 1$, we refer to it as the anti-bunching effect, while the case $g^{(2)} > 1$ is termed as bunching. $g^{(2)} = 1$ signifies that the measures of two particles at positions x_1 and x_2 are stochastically independent.

4 Results

To compare the results of dipolar interaction with the contact one, we fix the interaction strength g_d and λ requiring the effective interaction

$$\int \frac{1}{x^3 + \alpha} dx = \int \delta(x) dx = 1, \qquad (17)$$

so that the integral of $\hat{V}$ is the same with $\lambda = g_d$ in our units. equation (17) fixes as well the cut-off parameter α. Throughout the computation we keep a number M of orbitals which are sufficient to get convergence in the measured quantities (for $N = 4$, $M = 12$ orbitals are enough). The convergence is further guaranteed when the occupation in the last orbital is negligible. We prepared the ground state of the non-interacting Hamiltonian using the R-MCTDHB package [66,83,123,124]. The interactions are then abruptly turned on at $t = 0$.

In Figure 1, we plot the natural occupations n_j as a function of time. The left panel is for contact interaction and right panel is for dipolar interaction. We choose $g_d = \lambda = 5$. Initially at $t = 0$, only the first natural orbital contributes. When the time goes on, the occupation of the higher orbitals start to contribute. However we get a clear difference with time between the contact and the dipolar

interactions. For contact interaction, mostly one natural occupation, n_1, dominates throughout the time evolution and other occupations remain comparatively small. At variance, for dipolar interaction, again initially at time $t = 0$ only n_1 contributes, but at short time n_1 sharply decreases and other orbitals start to populate. For the rest of evolution we find that several other orbitals almost equally contribute as n_1 (we checked that the obtained results do not depend on the chosen value of M). However, with the considered number of particles our present computation is unable to present the full-blown N-fold occupation of natural orbitals which can be achieved when the system is quenched to very large values of g_d, that correspond to crystal-like states [125,126]; required orbitals are too large to achieve the convergence.

Figure 2 reports the dynamics of many-body SIE for dipolar as well as for contact interactions. The statistical relaxation is manifested by the long-time dynamics when $S^{\text{info}}(t)$ saturates to a maximum entropy state. At very short time we observe linear increase in $S^{\text{info}}(t)$ fitted with the analytical formula $S = \Gamma t \ln P$, where Γ is determined by the decay probability to stay in the initial ground state and P is the number of many-body states [127,128]. However the difference in $S^{\text{info}}(t)$ for contact and dipolar interactions can be identified from the corresponding Γ values. For contact interaction the linear increase is determined by Γ_c which is significantly smaller than the corresponding Γ_d for dipolar interaction. The very sharp linear increase in the information entropy for dipolar interaction implies the number of principal components participating in the many-body dynamics increases exponentially very fast. At long times, the system relaxes to the maximum entropy state. For contact interaction, $S^{\text{info}}(t)$ also has a tendency to achieve a saturation value or maximum entropy value, however the corresponding Γ value (Γ_c) is almost 125 times smaller than the Γ_d value - this implies very slow relaxation process. The saturation value or maximum entropy value achieved by the system for contact interaction is also smaller than that for the dipolar interaction.

In Figure 3, we present the time evolution of $S^{\text{occu}}(t)$ for the same interaction quench parameter as reported in Figure 2. At $t = 0$, when all bosons are in the lowest orbital : $n_1 = N = 4$ and all other $n_j = 0$, so $S^{\text{occu}}(t = 0) = 0$. At later time, the bosons are distributed in several orbitals as the many-body state is fragmented. Unlike $S^{\text{info}}(t)$, we observe significant difference in the dynamical evolution of $S^{\text{occu}}(t)$ for dipolar interaction compared to the contact interaction. The qualitative behaviour of $S^{\text{info}}(t)$ and $S^{\text{occu}}(t)$ for dipolar interaction is same only the maximum value of the entropy differes : $S^{\text{info}}_{\text{sat}} = 6.80$ and $S^{\text{occu}}_{\text{sat}} = 2.47$. However, $S^{\text{occu}}(t)$ for contact interaction exhibits rigorous fluctuation at short and intermediate time, the fluctuation gradually reduces. At long time (not shown here) it saturates to a maximum value.

The time evolution of information entropy $S^{\text{info}}(t)$ for other interaction quench (small values) is presented in Figure 4. The top panel corresponds to dipolar interaction and bottom panel corresponds to contact interaction ($g_d = \lambda = 0.1, 0.2, 0.5, 1.0$). In all cases the system is initially prepared in the noninteracting limit and then
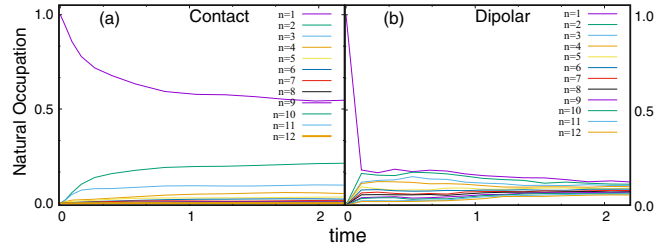

Fig. 1. Eigenvalues of the reduced density matrix (i.e., the natural occupations) as a function of time for $g_d = \lambda = 5$. Panel(a): contact interaction. Panel(b): dipolar interaction. The natural occupations n_j exhibit depletion for contact interactions (many small n_j with $j > 1$ emerge) and full-blown N-fold fragmentation for dipolar interactions (all n_j with $j \leq N$ contribute equally). All quantities shown are dimensionless.

suddenly quenched. For dipolar interaction, the qualitative nature of $S^{\text{info}}(t)$ is similar to Figure 2 - although for very small interaction quench we observe flat increase in $S^{\text{info}}(t)$ as Combine as expected, whereas, for contact interaction we observe very small production of entropy and there is no genuine signature of linear increase in $S^{\text{info}}(t)$ except $\lambda = 1.0$. The small interaction quench basically acts as a small external perturbation. We observe the same behaviour in $S^{\text{occu}}(t)$ (not shown here) for small interaction quenches.

Figure 5 presents the time evolution of the first-order correlation function $|g^{(1)}(x_1, x'_1; t)|^2$ as a function of its two spatial variables x_1 and x'_1 for various time t and fixed interaction strength quench. For contact interaction, $|g^{(1)}(x_1, x'_1; t)|^2$ remains close to unity for all (x_1, x'_1) for a comparatively long time. This implies that the system remains coherent. At longer time the off-diagonal correlation is gradually lost and finally at time $t = 1.0$ only the diagonal correlation is maintained. The strong interparticle repulsion leads to the loss of coherence which is further maintained at larger timescale when the system reaches to its relaxed state. It is also in good agreement with the relaxation process when $S^{\text{info}}(t)$ saturates to maximum entropy state. In contrast, for dipolar interaction we observe very quick loss of off-diagonal correlation. $|g^{(1)}(x_1, x'_1; t)|^2$ is close to unity almost exclusively for $x_1 = x'_1$, away from the diagonal ($x_1 \neq x'_1$) is close to zero. This is the effect of long-range repulsive tail of the dipolar interaction. Thus the relaxed state can be described as a many-body state with many natural orbitals occupied, maximum entropy and persistence of diagonal first-order correlation.

In Figure 6, we plot the corresponding second-order correlation function $g^{(2)}(x_1, x_2; t)$ for the same parameters as reported in Figure 5. At small time, for almost all (x_1, x_2) the second-order coherence is maintained for contact interaction, whereas the diagonal coherence starts to deplete for dipolar interaction. For larger times (such $t = 1$), $g^{(2)}(x_1, x_2; t) \approx 1$ at the off-diagonal ($x_1 \neq x_2$) for contact interaction, whereas the diagonal is almost vanishing. It means that there is a finite probability of detecting two particles for all (x_1, x_2), except for the narrow
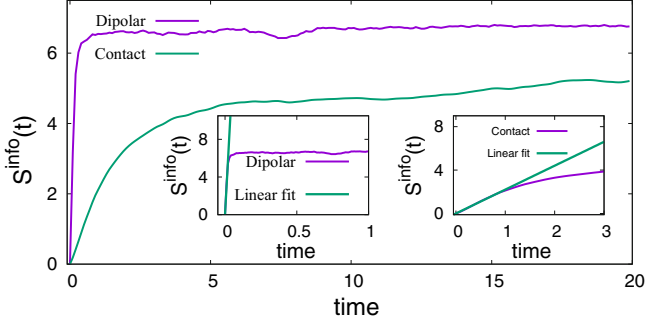
Fig. 2. Dynamics of $S^{\mathrm{info}}(t)$ or C-SIE for the same interaction quench as reported in Figure 1. The statistical relaxation is seen by the saturation of $S^{\mathrm{info}}(t)$ to the maximum entropy value. The insets present the sharp linear increase fitted with the analytical formula for small times (see text). Fitting parameters : $\Gamma_c = 0.34$ for contact interaction and $\Gamma_d = 43.2$ for dipolar interaction. All quantities shown are dimensionless.
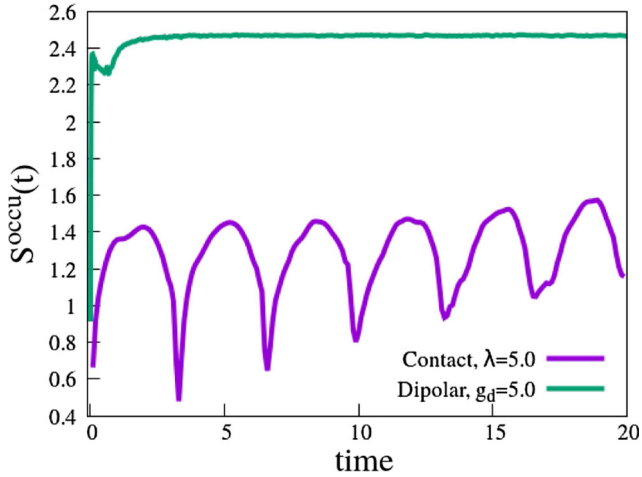

Fig. 3. Dynamics of $S^{\mathrm{occu}}(t)$ or O-SIE for the same interaction quench as reported in Figure 1. The statistical relaxation is seen by the saturation of $S^{\mathrm{occu}}(t)$ to the maximum entropy value for dipolar interaction. For contact interaction the fluctuations present in the occupation entropy reduces slowly with time. At very long time the system will relax. All quantities shown are dimensionless.

Fig. 4. Dynamics of $S^{\mathrm{info}}(t)$ for small interaction quenches. Top panel is for dipolar interaction. The qualitative behaviour for all the small interaction quenches are almost same. Bottom panel is for contact interaction. These small quenches act as perturbation. All quantities shown are dimensionless.

band around the diagonal. The vanishing diagonal part of $g^{(2)}(x_1, x_2; t)$ is corresponding to the anti-bunching effect, as the probability of finding a double occupation along the diagonal is almost zero. Complete vanishing of the diagonal coherence is maintained at larger times. For dipolar interaction, the anti-bunching effect appears at very short times such $t \approx 0.01$. With further increase in time, the anti-bunching band spreads. The quick development of the anti-bunching effect for dipolar interaction is also in good agreement with our previous observation [129] when $S^{\mathrm{info}}(t)$ quickly attains the saturation value. We conclude that by observing very quick loss of first-order coherence and the setup of the anti-bunching effect in second-order coherence may be considered as characterizing the many-body state with maximum entropy. Since with further increase in time we do not observe any change in entropy
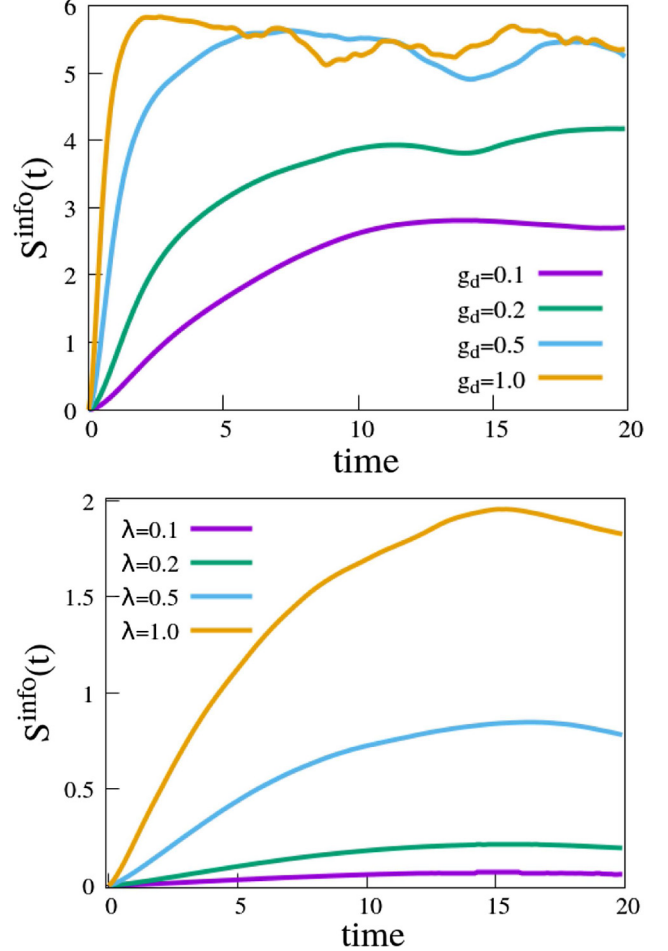
production, first- and second-order correlation functions, we may define the state as a relaxed state. As the different orders of coherence can be measured experimentally the above relation between the entropy production and coherence can be directly verified in the experiment to test the process of statistical relaxation. All our results presented here can be measured experimentally using single-shot absorption imaging [130–134]. From experimental absorption images, the one-body and two-body density are available as averages of many single-shot images. In the present work, we have calculated first- and second-order correlation functions using one- and two-body density. Thus a direct verification of our results can be performed easily. Furthermore, references [97,125] suggest that the natural occupations can be inferred from the integrated variance of single-shot images, at least at zero temperature.

Our present calculation is done for a finite system of few particles. The natural question is to verify our present observation for larger bosonic systems. In our previous work [129], we have already reported the quench dynamics with contact interaction for a larger number of bosons,
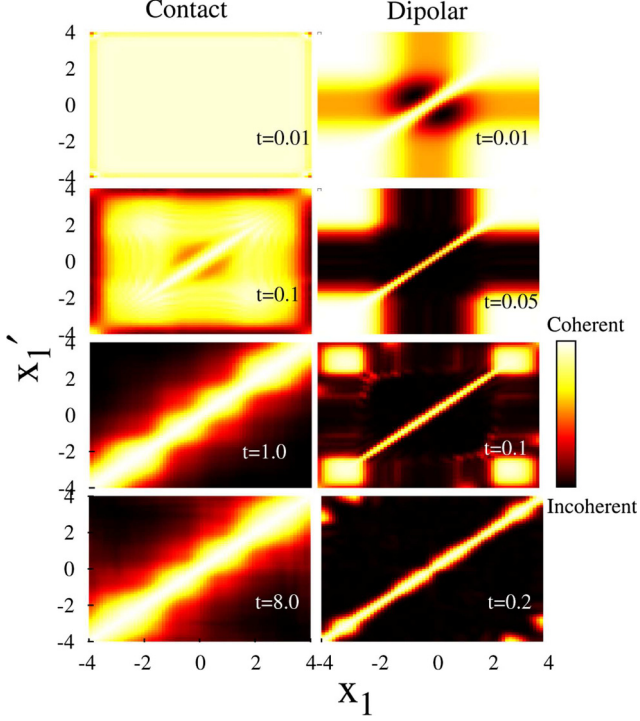
6

Fig. 5. Coherence in the quench dynamics measured with first-order correlation function $|g^{(1)}(x_1, x_1'; t)|^2$. The left column depicts $|g^{(1)}|^2$ for contact interaction for the times $t = 0.01, 0.1, 1.0$ and 8.0 respectively. The right column shows the same for dipolar interaction for time $t = 0.01, 0.05, 0.1$ and 0.2 respectively. For the dipolar interaction $|g^{(1)}|^2$ becomes close to zero almost everywhere except the diagonal at very short time, in good agreement with the quick and large production of the many-body SIE. All quantities shown are dimensionless.

Fig. 6. Coherence in the quench dynamics measured with second-order correlation function $g^{(2)}(x_1, x_2; t)$. The left column depicts $g^{(2)}$ for contact interaction for time $t = 0.01, 0.1, 1.0$ and 8.0 respectively. The right column shows the same for dipolar interaction for time $t = 0.01, 0.05, 0.1$ and 0.2 respectively. For dipolar interaction the diagonal part of $g^{(2)}$ is extinguished quickly due to the repulsive long-range tail and the anti-bunching effect develops in correspondence of the behaviour of the SIE. All quantities shown are dimensionless.

however only the first-order correlation dynamics and its link with the production of entropy have been discussed. In the context of our present computation we redo the simulation for $N = 10$ bosons with contact interaction and observed the similar physics in the second-order correlation dynamics as observed for $N = 4$ bosons. However we are unable to extend our simulation for $N = 10$ bosons with dipolar interaction due to serious convergence problem. Increasing the particle number increases the size of the Hilbert space rapidly. For example, for $N = 4$ bosons distributed over $M = 12$ orbitals the size of the Hilbert space is $N_{conf} = 1365$ and the same for $N = 10$ bosons is 352716. However for 10 bosons, with dipolar interaction $M = 12$ orbitals may not be sufficient to achieve convergence. So we checked our present observations for $N = 6$ bosons distributed in $M = 15$ orbitals and the general conclusion drawn for $N = 4$ dipolar bosons remain unchanged.

5 Conclusion

In this paper, we considered few dipolar bosons in a 1D harmonic trap. We studied the statistical relaxation of dipolar boso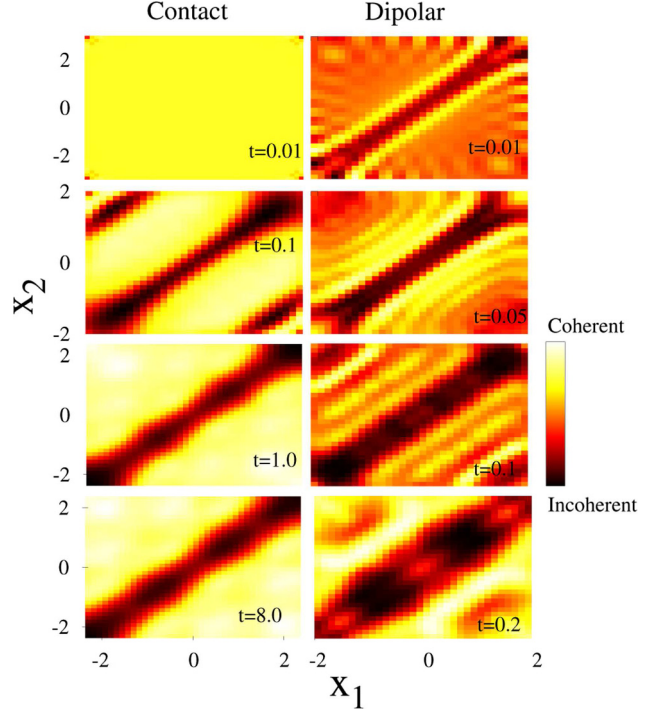ns and its comparison with that for contact interaction. We solved the quantum many-body dynamics by MCTDHB and the relaxation is presented through the time evolution of natural occupation, entropy production, normalized first- and second-order Glauber's correlation functions. In the long time dynamics, the system relaxes to its maximum entropy state. The effect of the long-range repulsive tail of dipolar interaction in the dynamics is clearly visible. The relaxation process for dipolar interaction is quicker than that for contact interaction. We also presented a link between the production of entropy and the first- and second-order coherences. We observed that at the time when the many-body system occupies many natural orbitals, then at the same time the off-diagonal coherence in first-order correlation function is completely lost, and the anti-bunching effect is exhibited in the second-order correlation. Thus in our present work, we redefine the relaxed state as the many-body state with maximum entropy retaining only the diagonal correlation in $g^{(1)}$ and developing the anti-bunching effect in $g^{(2)}$. Two remaining and natural open questions are to study the connection of these results with the behaviour of collective modes and to consider the broader class of long-range interactions with smaller power of interaction, especially when its value is smaller than the dimension of the considered system.

Author contribution statement

S. Bera conducted the numerical and theoretical investigations, S. Bera, B. Chakrabarti, S.K. Haldar, A. Trombettoni and V.K.B. Kota wrote the manuscript, conceived the idea for the project and supported the write up.

References

1. A.M. Kaufman, M.E. Tai, A. Lukin, M. Rispoli, R. Schittko, P.M. Preiss, M. Greiner, Science **353**, 794 (2016)
2. S. Trotzky, Y.A. Chen, A. Flesch, I.P. McCulloch, U. Schollwöck, J. Eisert, I. Bloch, Nat. Phys. **8**, 325 (2012)
3. M. Cheneau, P. Barmettler, D. Poletti, M. Endres, P. Schaua, T. Fukuhara, C. Gross, I. Bloch, C. Kollath, S. Kuhr, Nature **481**, 484 (2012)
4. T. Kinoshita, T. Wenger, D.S. Weiss, Nature **440**, 900 (2006)
5. M. Greiner, O. Mandel, T.W. Hänsch, I. Bloch, Nature **419**, 51 (2002)
6. S. Will, T. Best, U. Schneider, L. Hackermuller, D. Luhmann, I. Bloch, Nature **465**, 197 (2002)
7. T. Langen, R. Geiger, M. Kuhnert, B. Rauer, J. Schmiedmayer, Nat. Phys. **9**, 640 (2013)
8. T. Langen, S. Erne, R. Geiger, B. Rauer, T. Schweigler, M. Kuhnert, W. Rohringer, I.E. Mazets, T. Gasenzer, J. Schmiedmayer, Science **348**, 207 (2015)
9. M. Gring, M. Kuhnert, T. Langen, T. Kitagawa, B. Rauer, M. Schreitl, I. Mazets, D.A. Smith, E. Demler, J. Schmiedmayer, Science **337**, 1318 (2012)
10. A. Minguzzi, D.M. Gangardt, Phy. Rev. Lett. **94**, 240404 (2005)
11. M. Collura, S. Sotiriadis, P. Calabrese, Phy. Rev. Lett. **110**, 245301 (2013)
12. L.F. Santos, F. Borgonovi, F.M. Izrailev, Phys. Rev. E **85**, 036209 (2012)
13. L.F. Santos, F. Borgonovi, F.M. Izrailev, Phys. Rev. Lett. **108**, 094102 (2012)
14. F.M. Izrailev, A. Castañeda-Mendoza, Phys. Lett. A **350**, 355 (2006)
15. M. Horoi, V. Zelevinsky, B.A. Brown, Phys. Rev. Lett. **74**, 5194 (1995)
16. N. Frazier, B.A. Brown, V. Zelevinsky, Phys. Rev. C **54**, 1665 (1996)
17. V.V. Flambaum, F.M. Izrailev, G. Casati, Phys. Rev. E **54**, 2136 (1996)
18. V.V. Flambaum, F.M. Izrailev, Phys. Rev. E **55**, R13 (1997)
19. V.V. Flambaum, F.M. Izrailev, Phys. Rev. E **56**, 5144 (1997)
20. F.M. Izrailev, Phys. Scr. **T90**, 95 (2001)
21. A. Polkovnikov, K. Sengupta, A. Silva, M. Vengalattore, Rev. Mod. Phys. **83**, 863 (2011)
22. V.K.B. Kota, A. Relaño, J. Retamosa, M. Vyas, J. Stat. Mech. **2011**, P10028 (2011)
23. S.R. Manmana, S. Wessel, R.M. Noack, A. Muramatsu, Phys. Rev. Lett. **98**, 210405 (2007)
24. G. Roux, Phys. Rev. A **79**, 021608R (2009)
25. F. Borgonovi, F.M. Izrailev, L.F. Santos, V.G. Zelevinsky, Phys. Rep. **626**, 1 (2016)
26. L.M. Duan, E. Demler, M.D. Lukin, Phys. Rev. Lett. **91**, 090402 (2003)
27. S. Trotzky, P. Cheinet, S. Fölling, M. Feld, U. Schnorrberger, A.M. Rey, A. Polkovnikov, E.A. Demler, M.D. Lukin, I. Bloch, Science **319**, 295 (2008)
28. T.C. Hsu, J. C. Anglès d'Auriac, Phys. Rev. B **47**, 14291 (1993)
29. J. Simon, W.S. Bakr, R. Ma, M.E. Tai, P.M. Preiss, M. Greiner, Nature **472**, 307 (2011)
30. Y.A. Chen, S. Nascimbene, M. Aidelsburger, M. Atala, S. Trotzky, I. Bloch, Phys. Rev. Lett. **107**, 210405 (2011)
31. F. Dukesz, M. Zilbergerts, L.F. Santos, New J. Phys. **11**, 043026 (2009)
32. L.F. Santos, J. Phys. A **37**, 4723 (2004)
33. D.A. Rabson, B.N. Narozhny, A.J. Millis, Phys. Rev. B **69**, 054403 (2004)
34. Y. Avishai, J. Richert, R. Berkovits, Phys. Rev. B **66**, 052416 (2002)
35. K. Kudo, T. Deguchi, J. Phys. Soc. Jpn. **74**, 1992 (2005)
36. J.M. Deutsch, Phys. Rev. A **43**, 2046 (1991)
37. M. Srednicki, Phys. Rev. E **50**, 888 (1994)
38. M. Rigol, V. Dunjko, M. Olshanii, Nature **452**, 854 (2008)
39. L.F. Santos, M. Rigol, Phys. Rev. E **82**, 031130 (2010)
40. M. Rigol, L.F. Santos, Phys. Rev. A **82**, 011604(R) (2010)
41. M. Rigol, Phys. Rev. Lett. **103**, 100403 (2009)
42. L.F. Santos, M. Rigol, Phys. Rev. E **81**, 036206 (2010)
43. F. Anza, V. Vedral, Sci. Rep. **7**, 44066 (2017)
44. F. Anza, C. Gogolin, M. Huber, Phys. Rev. Lett. **120**, 150603 (2018)
45. D. Vodola, L. Lepori, E. Ercolessi, A.V. Gorshkov, G. Pupillo, Phys. Rev. Lett. **113**, 156402 (2014)
46. Z.X. Gong, M.F. Maghrebi, A. Hu, M. Foss-Feig, P. Richerme, C. Monroe, A.V. Gorshkov, Phys. Rev. B **93**, 205115 (2016)
47. L. Lepori, D. Vodola, G. Pupillo, G. Gori, A. Trombettoni, Ann. Phys. **374**, 35 (2016)
48. G.L. Celardo, R. Kaiser, F. Borgonovi, Phys. Rev. B **94**, 144206 (2015)
49. N. Defenu, A. Trombettoni, S. Ruffo, Phys. Rev. B **94**, 224411 (2016)
50. L. Lepori, A. Trombettoni, D. Vodola, J. Stat. Mech. 033102, (2017)
51. N. Defenu, A. Trombettoni, S. Ruffo, Phys. Rev. B **96**, 104432 (2017)
52. F. Iglói , B. Blaβ, G. Roósz, H. Rieger, Phys. Rev. B **98**, 184415 (2018)
53. B. Blaβ, H. Rieger, G. Roósz, F. Iglói, Phys. Rev. Lett. **121**, 095301 (2018)
54. N. Defenu, T. Enss, M. Kastner, G. Morigi, Phys. Rev. Lett. **121**, 240403 (2018)
55. L. Lerose, B. Zunkovic, A. Silva, A. Gambassi, Phys. Rev. B **99**, 121112(R) (2019)

56. M.A. Baranov, M. Dalmonte, G. Pupillo, P. Zoller, Chem. Rev. **112**, 5012 (2012)

57. D.S. Petrov, G.V. Shlyapnikov, J.T.M. Walraven, Phys. Rev. Lett. **85**, 3745 (2000)

58. V. Dunjko, V. Lorent, M. Olshanii, Phys. Rev. Lett. **86**, 5413 (2001)

59. Y. Tang, W. Kao, K.Y. Li, S. Seo, K. Mallayya, M. Rigol, S. Gopalakrishnan, B.L. Lev, Phys. Rev. X **8**, 021030 (2018)

60. M. Olshanii, Phys. Rev. Lett. **81**, 938 (1998)

61. S. Sinha, L. Santos, Phys. Rev. Lett. **99**, 140406 (2007)

62. A.I. Streltsov, O.E. Alon, L.S. Cederbaum, Phys. Rev. Lett. **99**, 030402 (2007)

63. O.E. Alon, A.I. Streltsov, L.S. Cederbaum, Phys. Rev. A **77**, 033613 (2008)

64. A. Lode, C. Lévêque, L. Madsen, A. Streltsov, O.E. Alon, arXiv:1908.03578 (2019)

65. K. Sakmann, *Many-Body Schrödinger Dynamics of Bose-Einstein Condensates, Springer Theses* (Springer, Heidelberg, 2011)

66. A.U.J. Lode, *Tunneling Dynamics in Open Ultracold Bosonic Systems, Springer Theses* (Springer, Heidelberg, 2014)

67. D. Iyer, N. Andrei, Phys. Rev. Lett. **109**, 115304 (2012)

68. M. Kormos, A. Shashi, Y.Z. Chou, J.S. Caux, A. Imambekov, Phys. Rev. B **88**, 205131 (2013)

69. M. Kormos, M. Collura, P. Calabrese, Phys. Rev. A **89**, 013609 (2014)

70. P.P. Mazza, M. Collura, M. Kormos, P. Calabrese, J. Stat. Mech. **2014**, P11016 (2014)

71. S. Sotiriadis, P. Calabrese, J. Stat. Mech. **2014**, P07024 (2014)

72. F. Franchini, A. Gromov, M. Kulkarni, A. Trombettoni, J. Phys. A: Math. Theor. **48**, 28FT01 (2015)

73. M. Collura, M. Kormos, P. Calabrese, J. Stat. Mech. **2014**, P01009 (2014)

74. L. Piroli, P. Calabrese, F.H.L. Essler, Phys. Rev. Lett. **116**, 070408 (2016)

75. S. Sotiriadis, Phys. Rev. A **94**, 031605(R) (2016)

76. F. Franchini, M. Kulkarni, A. Trombettoni, New J. Phys. **18**, 115003 (2016)

77. V. Alba, P. Calabrese, SciPost Phys. **4**, 017 (2018)

78. M. Collura, M. Kormos, P. Calabrese, Phys. Rev. A **97**, 033609 (2018)

79. W.S. Bakr, A. Peng, M.E. Tai, R. Ma, J. Simon, J. Gillen, S. Foelling, L. Pollet, M. Greiner, Science **329**, 547 (2010)

80. C.L. Hung, X. Zhang, L.C. Ha, S.K. Tung, N. Gemelke, C. Chin, New J. Phys. **13**, 075019 (2011)

81. M.D. Girardeau, E.M. Wright, Phys. Rev. Lett. **84**, 5239 (2000)

82. A.U.J. Lode, K. Sakmann, O.E. Alon, L.S. Cederbaum, A.I. Streltsov, Phys. Rev. A **86**, 063606 (2012)

83. E. Fasshauer, A.U.J. Lode, Phys. Rev. A **93**, 033635 (2016)

84. L. Cao, S. Krönke, O. Vendrell, P. Schmelcher, J. Chem. Phys. **139**, 134103 (2013)

85. R. Schmitz, S. Krönke, L. Cao, P. Schmelcher, Phys. Rev. A **88**, 043601 (2013)

86. U.R. Fischer, A.U.J. Lode, B. Chatterjee, Phys. Rev. A **91**, 063621 (2015)

87. R. Roy, A. Gammal, M.C. Tsatsos, B. Chatterjee, B. Chakrabarti, A.U.J. Lode, Phys. Rev. A **97**, 043625 (2018)

88. S.K. Haldar, O.E. Alon, Chem. Phys. **509**, 72 (2018)

89. S.K. Haldar, O.E. Alon, J. Phys.: Conf. Ser. **1206**, 012010 (2019)

90. S.K. Haldar, O.E. Alon, New J. Phys. **21**, 103037 (2019)

91. O.E. Alon, J. Phys.: Conf. Ser. **1206**, 012009 (2019)

92. J. Grond, J. Schmiedmayer, U. Hohenester, Phys. Rev. A **79**, 021603(R) (2009)

93. J. Grond, T. Betz, U. Hohenester, N.J. Mauser, J. Schmiedmayer, T. Schumm, New J. Phys. **13**, 065026 (2011)

94. R. Beinke, S. Klaiman, L.S. Cederbaum, A.I. Streltsov, O.E. Alon, Phys. Rev. A **92**, 043627 (2015)

95. J.M. Schurer, A. Negretti, P. Schmelcher, New J. Phys. **17**, 083024 (2015)

96. A.U.J. Lode, C. Bruder, Phys. Rev. A **94**, 013616 (2016)

97. A.U.J. Lode, C. Bruder, Phys. Rev. Lett. **118**, 013603 (2017)

98. C. Lévêque, L.B. Madsen, New J. Phys. **19**, 043007 (2017)

99. G.C. Katsimiga, S.I. Mistakidis, G.M. Koutentakis, P.G. Kevrekidis, P. Schmelcher, New J. Phys. **19**, 123012 (2017)

100. F. Dalfovo, S. Giorgini, L.P. Pitaevskii, S. Stringari, Rev. Mod. Phys. **71**, 463 (1999)

101. L. Pitaevskii, S. Stringari, *Bose-Einstein Condensation and Superfluidity* (Oxford University Press, Oxford, 2016)

102. P. Kramer, M. Saracento, *Geometry of the Time-dependent Variational Principle* (Springer, Berlin, 1981)

103. H.J. Kull, D. Pfirsch, Phys. Rev. E **61**, 5940 (2000)

104. P.O. Löwdin, Phys. Rev. **97**, 1474 (1955)

105. A.J. Coleman, V.I. Yukalov, Reduced density matrices: Coulson's challenge, in *Lectures notes in chemistry* (Springer, Berlin, 2000), Vol. 72

106. S.A. Rice, in *Reduced-density-matrix mechanics: With application to many-electron atoms and molecules*, edited by D.A. Mazziotti, Advances in Chemical Physics (Wiley, New York, 2007), Vol. 134

107. K. Sakmann, A.I. Streltsov, O.E. Alon, L.S. Cederbaum, Phys. Rev. A **78**, 023615 (2008)

108. O. Penrose, L. Onsager, Phys. Rev. **104**, 576 (1956)

109. P. Nozières, D. Saint James, J. Phys. **43**, 1133 (1982)

110. P. Nozières, in *Bose-Einstein condensation*, edited by A. Griffin, D.W. Snoke, S. Stringari (Cambridge University Press, Cambridge, England, 1996), p. 15

111. R.W. Spekkens, J.E. Sipe, Phys. Rev. A **59**, 3868 (1999)

112. E.J. Mueller, T.L. Ho, M. Ueda, G. Baym, Phys. Rev. A **74**, 033612 (2006)

113. S.E. Massen, C.P. Panos, Phys. Lett. A **246**, 530 (1998)

114. M. Rigol, Phys. Rev. Lett. **112**, 170601 (2014)

115. S.E. Massen, C.P. Panos, Phys. Lett. A **280**, 65 (2001)

116. S.E. Massen, Ch.C. Moustakidis, C.P. Panos, Phys. Lett. A **299**, 131 (2002)

117. S.E. Massen, Ch.C. Moustakidis, C.P. Panos, in *Focus on boson research*, edited by A.V. Ling (Nova, New York, 2005)

118. S.K. Haldar, B. Chakrabarti, Int. J. Mod. Phys. B **27**, 1350048 (2013)

119. S.K. Haldar, B. Chakrabarti, T.K. Das, A. Biswas, Phys. Rev. A **88**, 033602 (2013)

120. V.K.B. Kota, in *Embedded random matrix ensembles in quantum physics* (Springer), Vol. 884

121. O.E. Alon, A.I. Streltsov, L.S. Cederbaum, Phys. Lett. A **362**, 453 (2007)
122. R.J. Glauber, Phys. Rev. **130**, 2529 (1963)
123. A.U.J. Lode, M.C. Tsatsos, E. Fasshauer, R. Lin, L. Papariello, P. Molignini, C. Lévêque, MCTDH-X: The time-dependent multiconfigurational Hartree for indistinguishable particles software (2018), `http://ultracold.org`
124. A.U.J. Lode, Phys. Rev. A **93**, 063601 (2016)
125. B. Chatterjee, A.U.J. Lode, Phys. Rev. A **98**, 053624 (2018)
126. S. Bera, B. Chakrabarti, A. Gammal, M.C. Tsatsos, M.L. Lekala, B. Chatterjee, C. Lévêque, A.U.J. Lode, Sci. Rep. **9**, 17873 (2019)
127. V.V. Flambaum, F.M. Izrailev, Phys. Rev. E **64**, 036220 (2001)
128. S.K. Haldar, N.D. Chavda, M. Vyas, V.K.B. Kota, J. Stat. Mech.: Theory Exp. **2016**, 043101 (2016)
129. A.U.J. Lode, B. Chakrabarti, V.K.B. Kota, Phys. Rev. A **92**, 033622 (2015)
130. K. Sakmann, M. Kasevich, Nat. Phys. **12**, 451 (2016)
131. J. Javanainen, S.M. Yoo, Phys. Rev. Lett. **76**, 161 (1996)
132. Y. Castin, J. Dalibard, Phys. Rev. A **55**, 4330 (1997)
133. J. Dziarmaga, Z.P. Karkuszewski, K. Sacha, J. Phys. B **36**, 1217 (2003)
134. D. Dagnino, N. Barberán, M. Lewenstein, Phys. Rev. A **80**, 053611 (2009)